Journal of Ovonic Research Vol. 10, No. 5, September - October 2014, p. 175 - 184

SYNTHESIS AND CHARACTERIZATION OF ZINC SELENIDE (ZnSe) THIN FILMS ELECTRODEPOSITED ON ITO AND SnO_2SUBSTRATES

D. SARAVANAKKUMAR, M. KASHIF[a], V. RETHINASAMI,
B. RAVIKUMAR , S. PANDIARAJAN, A. AYESHAMARIAM[b*],
S. SIVARANJANI[c], M. BOUOUDINA[d,e] S.RAMALINGAM [f]

Department of Physics, Devanga Arts College (Auto), Aruppukkottai, Tamil Nadu, 626 101, India
[a]Department of electrical and electronic engineering, Faculty of engineering, Universiti Malayaia Sarawak 94300, Kota Samarahan Sarawak
[b]Department of Physics, Khadir Mohideen College, Adirampattinam, 614 701, India
[c]Department of Physics, SBM College of Engineering and technology, Dindigul-624 005, India
[d]Department of Physics, College of Science, University of Bahrain, PO Box 32038, Kingdom of Bahrain
[e]Nanotechnology Centre, College of Science, University of Bahrain, PO Box 32038, Kingdom of Bahrain
[f] Department of Physics, AVC College, Mayiladuthurai, Tamilnadu, India

The ZnSe thin films were deposited on ITO and SnO_2 substrates by modified-electro deposition method. In order to limit the particle size, the growth was controlled by stabilization of nanocrystals in ITO and SnO_2. The X-ray diffraction studies, laser Raman vibrational identification and photoluminescence analyses confirmed the formation of nano crystal (ZnSe) in simple cubic phase with a mean crystallite size 20 nm on both substrates. From the optical studies, it was observed that, the blue shift taking place in the optical absorption and the luminescence data is consistent with the reported values.

(Received June 29, 2014; Accepted October 11, 2014)

Keywords: Electrodeposition;ZnSe; Thin films; ITO; SnO_2

1. Introduction

The recent research on thin films has been stimulated by potential applications in light emitting devices, flat panel displays and blue light laser technology. In order to achieve quantum size effects, it is necessary to synthesize nanometer-size crystallites smaller than the exciton (electron-hole pair) diameter. The precipitation of quantum dots in the presence of confining media further allows better size control and stability. Some strategies employed to date include arrested nucleation in glasses [1–5], precipitation from sol–gel solutions [6] and entrapment in porous sites inside zeolite cavities [7]. The ZnSe material is used for short wavelength visible light lasers has stimulated interest to synthesis ZnSe nanoparticles in the quantum size regime. The ZnSe quantum dots have been prepared using an arrested precipitation colloidal technique [8], a sol–gel process [9] and arrested nucleation in glass [10].

BongHyun Boo et al., [11] have reported the crystalline ZnSe thin films doped with nitrogen have been grown on polished GaAs(100) and Si(100) substrates bypulsed laser ablation deposition (PLAD) in N_2 atmosphere. Atomic force microscopy (AFM) showed that the surface morphology was flat and dense, and the roughness with a roughness of about 1.3 nm for GaAs

*Corresponding author: aismma786@gmail.com

(100) in $2x10^3$ Torr N_2 ambient. The X-ray diffraction (XRD) analysis confirmed the formation of single crystalline epitaxial layer. AFM observations indicate that the crystallographic quality largely depends on ambient pressure and lattice mismatch. X-ray photoelectron spectroscopy demonstrates that Zn and Se atoms forZnSe film grown onto GaAs(100) at $2x10^3$Torr bond to each other and that the concentrations of [N] is7% and less than 3% for [O]without the presence of any impurities. The concentration of doped nitrogen for the best ZnSe thin film grown on GaAs(100) wasestimated to be over 1021 cm^{-3} [11].

Archanaet al. [12] reported that mono dispersed ZnSe nano wires (NWs) have been synthesized by wet chemical method using edamine as a surface capping ligand. Ultraviolet visible absorption spectrum confirms that the absorption edge is located at 371 nm which is blue shifted when compared to the value of bulk ZnSe. The photoluminescence spectrum showed that the emission peak is located at 442 nm which corresponds to near band edge emission. The NWs have a uniform average diameter of 80 nm and a length of about few μm. The presence of Edamine is confirmed by the Fourier transform spectrophotometer. The possible growth mechanism is also addressed as well [12].

Jianjunet al., [13] reported for the first time the fabrication of a very sensitive and simple electrochemical sensor for chlorophenols (CPs) based ona nano composite of cetyltri-methyl ammonium bromide (CTAB) and ZnSe quantum dots (ZnSe–CTAB)through electrostatic self-assembly technology. The composite of ZnSe–CTAB introduced a favorable access for the electron transfer and gave superior electro catalytic activity for the oxidation of CPs than ZnSe QDs and CTAB alone. Differential pulse voltametry (DPV) was used for the quantitative determination of the CPs including 2-chlorophenol (2-CP), 2,4-dichlorophenol (2,4-DCP) and pentachlorophenol (PCP). Under the optimum conditions, the peak currents of the CPs were proportional to their concentrations in the range from 0.02 to 10.0 mM for 2-CP, 0.006 to 9.0 mM for 2,4-DCP, and0.06 to 8.0 for PCP. The detection limits were 0.008 mM for 2-CP, 0.002 mM for 2,4-DCP, and 0.01 mMfor PCP, respectively [13].

P. Reiss et al. [14] reported a new synthesis method of colloidal ZnSe nano crystals exhibiting size-dependent optical properties is reported. The ZnSe quantum dots are prepared in a non-coordinating solvent (octadecane) via direct reaction of zinc stearate with selenium dissolved in trioctylphosphine, i.e., without the use of pyrophoric reagents. The photoluminescence of the resulting nanocrystals can be tuned in the spectral range 390–440 nm with constant emission line widths of the order of 15 nm [14].

Pushpendra et al., [15] reported a simple, effective and reproducible chemical synthetic route for the production of high-quality pure ZnSe nanoparticles (NPs) and lanthanum-doped ZnSe (ZnSe:La) NPs. The wide bandgap and luminescent pure ZnSe and ZnSe:La NPs have been synthesized at a low temperature (100°C) in a single template-free step. A broad photoluminescence (PL) emission across the visible spectrum has been demonstrated by a systematic blue-shift in emission due to the formation of NPs. It was observed that the contribution to the emission intensity from surface states of NPs increases with La doping. TEM data revealed that the average size of ZnSe and ZnSe:La NPs is 14 and 8 nm, respectively. On the other hand, band gap energy Eg of ZnSe and ZnSe:La NPs were found to be 3.59 eV and 3.65 eV, respectively. Results showed that hydrazine hydrate played multiple roles in the formation of ZnSe and ZnSe:La NPs. A possible reaction mechanism for the growth of NPs is also discussed [15].

After the through literature screening, there was no work has been carried out on nano ZnSe thin films. Hence, in this attempt, the preparation and thorough characterization towards the application of nano ZnSe thin films have been carried out. The stable ZnSe thin films prepared by physical route in the presence of a ITO and SnO_2 coating plates which limit particle growth.

2. Experimental

2.1 Thin Films Preparation

The Electro deposition technique was adopted for the preparation of Zinc selenide (ZnSe) thin films. The chemicals used for the preparation were analytical reagent grade (99 % purity, E-Merck). The electrochemical experiments were performed using a PAR scanning potentiostat (Model 362, EG&G) employing a three- electrode configuration, with indium doped tin oxide (ITO) and SnO_2 glass substrates as cathode, graphite plate as anode and saturated calomel electrode (SCE) as reference electrode. The saturated calomel electrode was introduced into the solution by login capillary whose tip was placed as close as possible to the working electrode. All the experimental potentials referred to this electrodeare reported elsewhere [16].

An aqueous electrolytic solution containing 250 mM of $Zn(NO_3).2H_2O$ and 2.5 mM of $SeO_2$was prepared. Preliminary results revealed that when the $Zn(NO_3).2H_2O$ concentration is kept below 200 mM there is no incorporation of Zn ions into the film, while for 250 mMand above, there is an excess of Zn content in the films. Additionally, it was observed that for a very low pH<3.5 value, the films grow spontaneously at high current densities making the process uncontrollable. The rapid growth of films followed by its peeling out from the substrate is observed.For a pH>3.5, the precipitation of $ZnSO_4$ occurs in the deposition bath. At pH value around 2.5±0.1, the growth of films is most likely controllable with a current density around10 $mA.cm^{-2}$. Hence, the optimum value of pH for all depositions was fixed at 2.5±0.1. The deposition timewas optimized at 5, 10 and 15 minutes, uniform and adherent films were obtained. The potential of the electrolytic bath was increased or decreased in the range -750 mV to -650 mV. When the potential is increased to -750 mV then decreased below -650 mV, a rapid growth of the film was observed followed by belling out from the substrate itself. Therefore, the potential was fixed at -700 mV versus SCE for all depositions. Finally, the optimum conditions to synthesize ZnSe thin films are identified as:

(i) Electrolyte concentration: 250 mM of $Zn(NO_3).2H_2O$, 2.5 mM of SeO_2
(ii) Solution pH: 3.0±0.1
(iii) Deposition potential:-700 mV versus SCEand
(iv)Different deposition time 5 min, 10 min and 15 min.

2.2 Characterization of ZnSe thin films

The thickness of the deposited films was estimated using 'stylus profilometer'. The X-ray patterns were recorded PAN alytical X'Pert Pro diffractometer equipped with Cu-Kα radiation (λ =1.54056 Å). The Morphological observations were carried out using Hitachi S-3400N scanning electron microscope (SEM). Varian Cary Eclipse spectrophotometer employing 15W Xe flash lamp was used for the photoluminescence studies. Laser Raman spectroscopy was carried out using Renishaw inVia Laser Raman spectrometer. Optical transmittance spectra were recorded using a JASCO-V-570 spectrophotometer.

3. Results and Discussion

3.1. Structural Characterization by X-ray diffraction (XRD)

The XRD patterns (Figs. 1a and 1b) showed the presence of some weak diffractions belonging most probably to ITO and SnO_2 pre-deposited layers along with a full-size halo setting within 2θ=15º-35° which means that the deposited ZnSe is in the amorphous state.

All the diffraction peaks of ZnSe are well assigned to simple cubic crystalline phase which was obtained by only one plane of (111) as in JCPDS file of 88-2345. From the Figure .1, it is noted that, the intensity of the Zn peaks decreases with doping time of deposition, ZnSe content and the full-width at half-maximum (FWHM) widths peaks changed with respect to time of deposition which indicates that crystalline size of the thin film equal to 21 nm as well. The

diffraction pattern corresponding to (111) cubic structures was obtained only for 15 min deposition time of thin film ZnSe. All the crystallite sizes were calculated by Scherrer equation from the average of three strongest peaks. The strongest peaks can be classified as (200) and (111) reflections from inter planes of ZnSe. The broadening of the peaks indicates the presence of nanometer scale particles.

The crystallite size was determined by means of the X-ray line broadening method using the Scherer equation [17]

$$D=\frac{0.94\,\lambda}{\beta\,\mathrm{Cos}\theta} \tag{1}$$

Where λ is the wavelength of CuKα radiation (λ= 0.154056 nm), is the full width at half β maximum (FWHM) of the *(hkl)* peak at the diffracting angle *hkl*2θ, the (111) peak is used to calculate the crystalline size D.

The presence of single sharp peak in the figure confirms the polycrystalline nature of the ZnSe thin film with high periodicity and crystallinity. The preferential orientation of the crystal plane (110) corresponds to the Bragg's reflection at 2θ = 30.02º instead of 2θ = 27.20º, it may be due to the deposition of ZnSe thinfilm on indium tin oxide plate and tin oxide plates.

The lattice parameter *a* of the deposited ZnSe thin film at room temperature is calculated using the formula for the cubic crystal structure. For the cubic crystal system, the lattice parameter *a* is related to *d* with the following equation

$$\frac{1}{d^2}=\frac{h^2+k^2+l^2}{a^2} \tag{2}$$

Where *h*, *k*, and *l* are all integers, *(hkl)* is the lattice plane index, *a* are lattice constants, d_{hkl} is distance between two consecutive planes. The lattice parameter *a* and the interplanar distance d calculated from the XRD patterns are a = 5.1493 A˚ respectively.

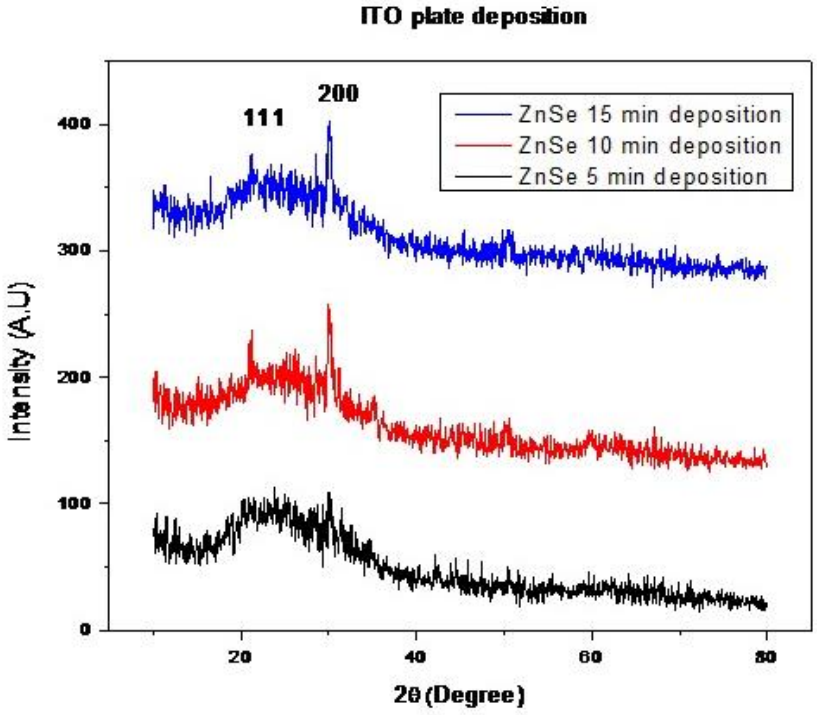

Fig.1a XRD pattern and variation of deposition time of ZnSe thin film deposited on ITO plate

But according to JCPDS file number 88-2345, the expected results of a = 5.670 A˚ for (111) plane and for SnO_2 plate 5.1479 A˚ for (111) plane. By utilizing the average crystallite size *D* [18], the size of ZnSe thinfilm nm in ITO plates and nearly the same nm in SnO_2 plates. If the deposited time for both the ITO and SnO_2 is raised from 5 min to 15 min in steps 5 min, we will get a preferential orientation along the (111) direction for both kinds of film for 15 min deposition shown in Fig 1a and Fig 1b, the structural parameters of these depositions are plotted in Table 1.

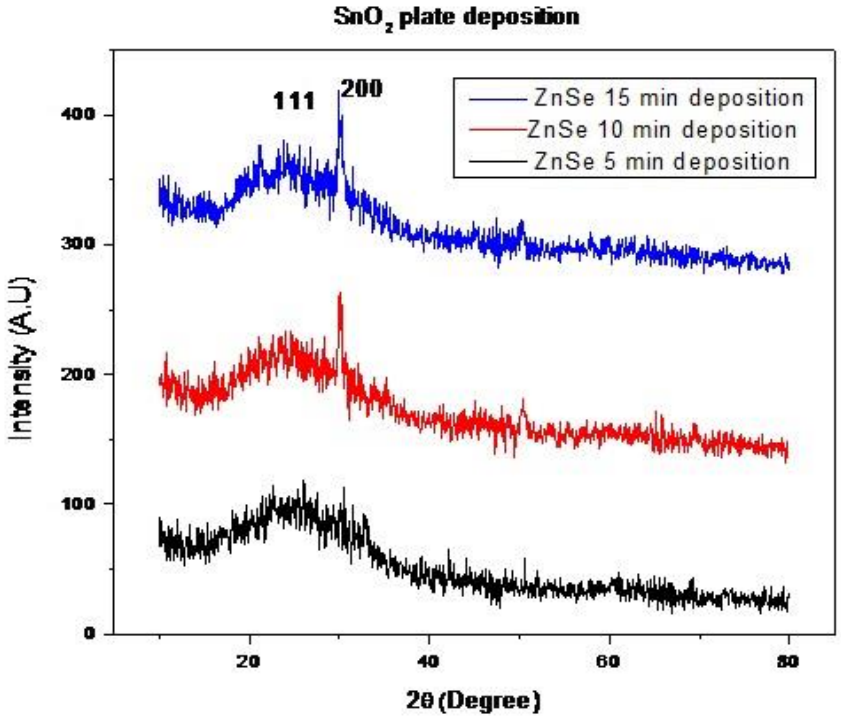

Fig. 1b XRD pattern and variation of deposition time of ZnSe thin films coated on SnO_2 plate

Table 1. Structural parameters of all films deposited in different deposition time

Samples	Crystallite size	Strain lines/m^2
ITO-1	8.23	0.0435
ITO-2	15.53	0.0454
ITO-3	20.069	-0.0354
SnO_2-1	4.114	-0.0399
SnO_2-2	19.72	-0.0476
SnO_2-3	20.07	0.0460

3.2 SEM Observations

The SEM images of ZnSe deposited onto ITO (Fig. 2(a-c)) reveals the formation of particles at the nano scale with homogeneous size distribution but with irregular shapes. No clear evidence on the effect of the deposition on both morphology or size of the particles can be clearly observed. Moreover, it can be observed that, the presence of high porosity, which means the formation of rough and non continuous SnSe thin film.

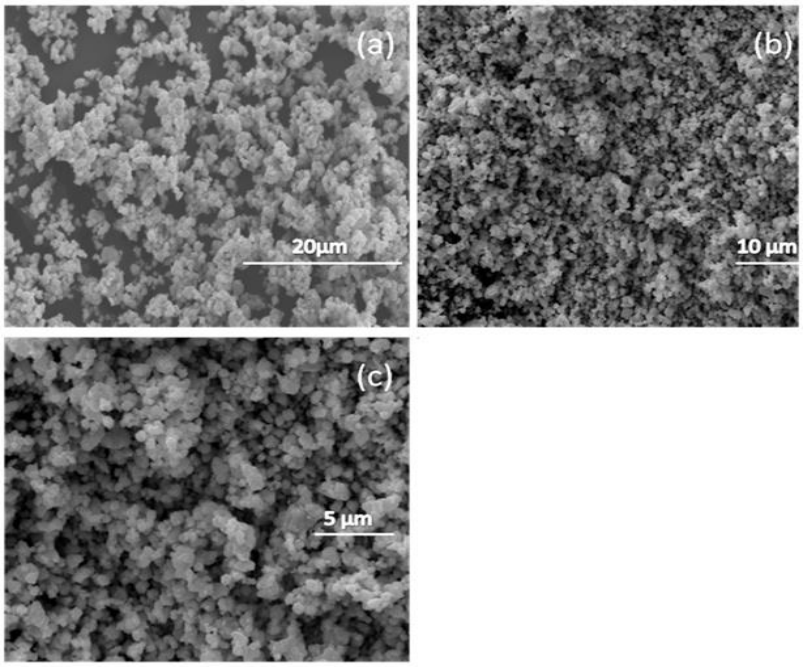

Fig. 2(a-c) Scanning Electron Microscopy (SEM) and variation of deposition time of ZnSe thin films deposited on ITO plate

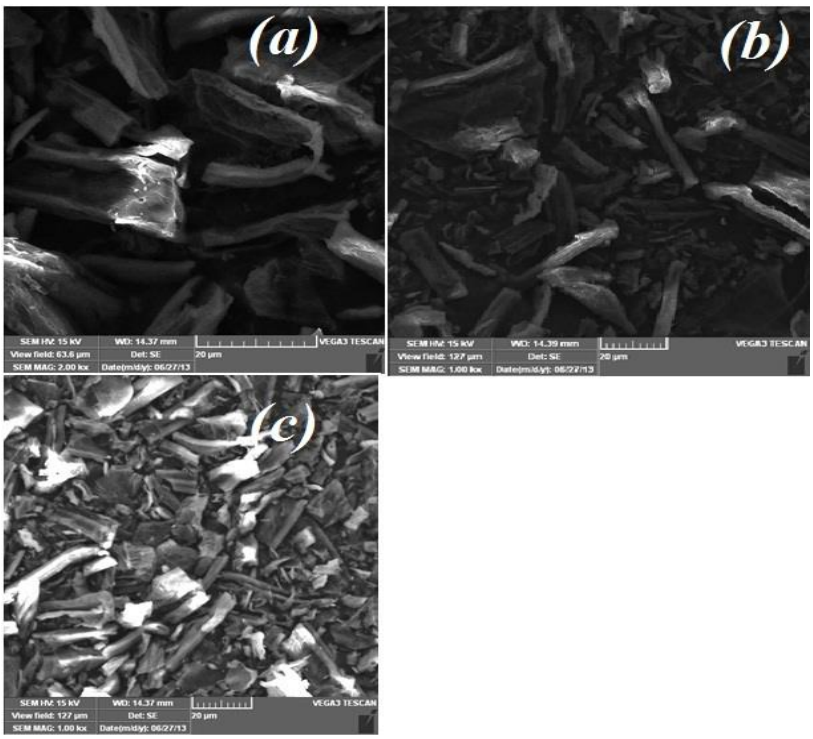

Fig. 3(a-c) Scanning Electron Microscopy (SEM) and variation of deposition time of ZnSe thin films deposited on SnO_2 plate

On the other hand, the SEM images of ZnSe deposited on SnO_2 (Fig. 3(a-c)) shows different type of microstructure which consisting of flakes-like shape, where both size and thickness are very considerably varied. It is important to mention that, the surface is dense and rough with less porosity.

3.3 Raman Spectroscopy Analysis

In Laser-Raman measurements, the spectra were taken at room temperature in a back scattering geometry with an allowed polarization configuration. The excitation radiation was at wavelength of 325 nm (eV) for which ZnSe is transparent. As seen from Fig. 4a, and Fig 4b, a large homogeneous broadening of Raman spectra at 689 and 828 cm^{-1} seems to be a common characteristic of nanomaterials with small crystallite sizes in the II–VI group. This view also observed in previous works [19,20]. The reduced dimensions of nanocrystals decrease the mean free path of phonons, and the phonons confined in the nanocrystals frequently collided and relaxed at the interface. Lattice distortion and structure defects are common features of most of the nano structured materials, which also result a shortening of the lifetime of phonons and contribute to the large homogeneous broadening [21,22].

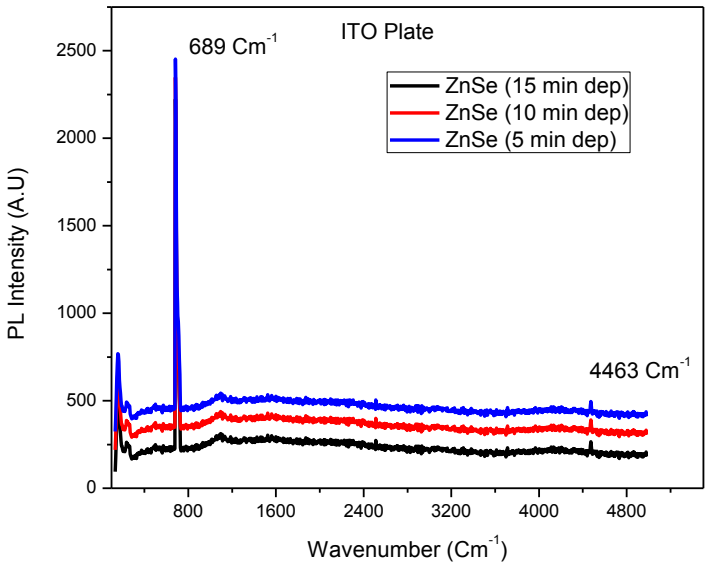

Fig. 4a Photoluminescence Spectra and variation of deposition time of ZnSe thin films deposited on ITO plate

As can be seen from Fig. 4a, and Fig 4b, and it was observed that, at different deposition time, the position of the 1LO and 2LO modes shifted from 510 to 689 cm^{-1} for ITO plate and 828 cm^{-1} for SnO_2 plate, from the values of bulk ZnSe [22], with a counter increase of full-width at half maximum (FWHM), which may be due to the nano size effect [19,20]. The intensity of the peaks also increases with increasing of deposition time of ZnSe on ITO and SnO_2 plates. For ITO plates, the ZnSe thin films emission peak is found at 689 cm^{-1} but for SnO_2 plate it was observed at 828 cm^{-1}.

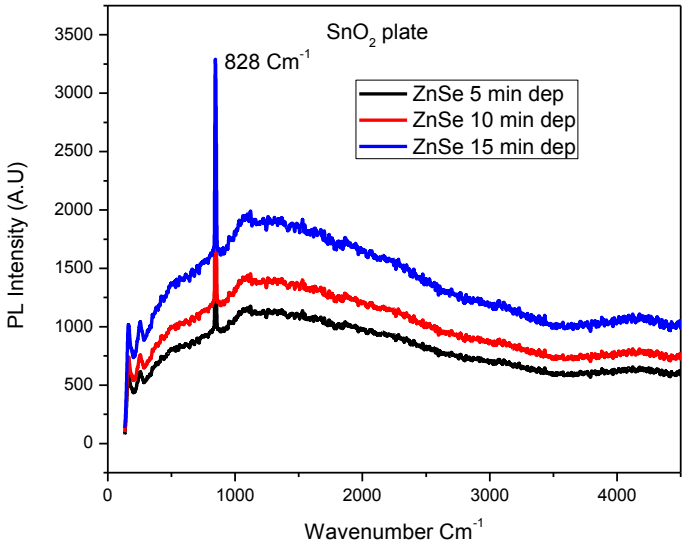

Fig. 4b laser Raman Spectra and variation of deposition time of ZnSe thin films deposited on ITO plate

3.4 Photoluminescence Analysis

The Fig. 5a and Fig. 5b exhibits the PL spectra of ZnSe thinfilms taken at room temperature. The absorption is blue shifted with respect to the different deposition time 5 min, 10 min and 15 min of ZnSe on ITO and SnO_2 plates, as would be expected for the smaller particle size. The excitonic absorption peaks are not very sharp but appear as broad humps due to different size distribution. For 15 min of deposition of ZnSe exhibits only one feature, one located near 689 nm for SnO_2 plate located at near 828 nm for ITO plate respectively as in Fig. 6. The stationary luminescence of ZnSe crystallites for both ITO and SnO_2 plates exhibits shifted gap for long time deposition (15 min) which are also shown in Fig 6 and Fig 7. These observations are consistent with the observed reduction in crystallite size of (20 nm) and this view also happened in the earlier report [23].

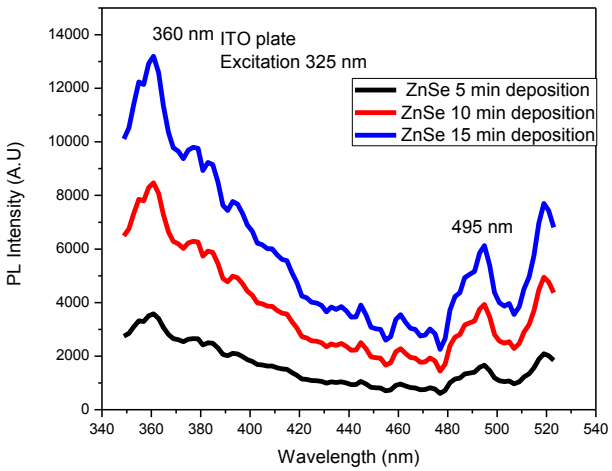

Fig. 5a Photoluminescence Spectra and variation of deposition time of ZnSe thin films deposited on ITO plate

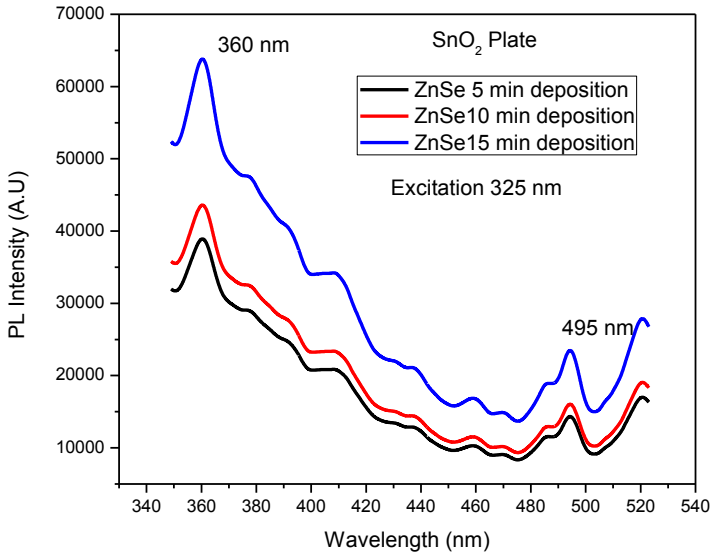

Fig. 5b laser Raman Spectra and variation of deposition time of ZnSe thin films deposited on SnO_2 plate

4. Conclusion

The well formed single crystal ZnSe thin films were obtained by the electro deposition method. From the deposition, it was found that the obtained crystallite sizes nearly 20 nm at the deposition time was increased from 5 min, 10 min and 15 min. the absorption and luminescence spectra displayed a blue shift of the material which was consistent with deposition time of ZnSe expected in this big size regime. The deposition of ZnSe on ITO and SnO_2 have limited crystallite sizes and enhanced stability of good emission peaks at the excitation of 325 nm. This provides an alternative to entrapment of shift when it was further annealed that samples to higher temperatures. It was also observed that, the ZnSe may be unsuitable for certain applications.

References

[1] A.I. Ekimov, A.A. Onushchenko, JETP Lett. **40**,1136 (1984).
[2] N.F. Borrelli, D.W. Hall, H.J. Holland, D.W. Smith, J. Appl.Phys. **61**,5399 (1987).
[3] B.G. Potter, J.H. Simmons, Phys. Rev. **B37**,10838 (1988).
[4] L.C. Liu, S.H. Risbud, J. Appl. Phys. 68,28 (1990).
[5] .C. Liu, S.H. Risbud, Philos. Mag. Lett. **61**,327 (1990).
[6] M. Nogami, K. Nagaska, E. Kato, J. Am. Ceram. Soc. **73,**2097 (1990).
[7] G.D. Stucky, J.E. Macdougall, Science **247**,669 (1990).
[8] N. Chestnoy, R. Hull, L.E. Brus, J. Chem. Phys. **85**,2237 (1986).
[9] G. Li, M. Nogami, J. Appl. Phys. **75**,4276 (1994).
[10] V.J. Leppert, S.H. Risbud, M.J. Fendorf, Philos. Mag. Lett. **75**,29 (1997).
[11] Bong Hyun Boo, KwangLee Ning Xu, Jae, Vacuum **64**,145 (2002).
[12] J. Archana, M. Navaneethan, S. Ponnusamy, Y. Hayakawa, C. Muthamizhcelvan, Letters **81**,59 (2012).
[13] Jianjun Li, Xiao Li, Ran Yang, Lingbo Qu, Peter de B. Harrington, AnalyticaChimicaActa **804**,76 (2013).
[14] P. Reiss, G. Quemard, S. Carayon, J. Bleuse, F. Chandezon, A. Pron, Materials Chemistry and Physics **84**,10 (2004).

[15] Pushpendra Kumar, Jai Singh, Mukesh Kumar Pandey , C.E. Jeyanthi, R. Siddheswaran, M. Paulraj , K.N. Hui, K.S. Hui, Materials Research Bulletin **49**,144 (2014).
[16] T. Mahalingam, R. Mariappan, V. Dhanasekaran, S. Mohan, G. Ravi, J.P.Chu, Chalcogenide Letters,**7**(12),669 (2010).
[17] T.Trindade, P O Brien,N L Pickett,Synthes.Chem. Mater.**13**,3843 (2001).
[18] R. E. Bailey, A M Smith,S Nie,PhysicaE **25**,1 (2004)
[19] P. Kumar, K. Singh, Cryst. Growth Des.**9,**3089 (2009).
[20] H. Young-Nam, P. Seung-Han, Phys. Rev. B **59**,7285 (1999).
[21] . Trallero-Giner, A. Debernardi, M. Cardona, Phys. Rev. B **57**,4664 (1998).
[22] L.D. Yao, F.F. Wang, X. Shen, S.J. You, L.X. Yang, S. Jiang, Y.C. Li, K. Zhu, Y.L. Liu, A.L. Pan, B.S. Zou, J. Liu, C.Q. Jin, R.C. Yu, J. Alloy Compd. **480**,798 (2009).
[23] A.V. Nurmikko, R.L. Gunshor, Physics and applications of II–VI quantum confined structures, in: F. Henneberger, S. Schmitt-Rink, E.O. Goberl (Eds.), Optics of Semiconductor Nanostructures, AkademieVerlag, Berlin, 1993, p. 240.